Synthesis characterization and sorption properties of nanoscale zero valent iron using red mud as the iron source: cadmium removal from spiked aqueous solutions

Despina Pentari[1]*, Afroditi Tournavitou [1] and Antonios Stratakis[1]

[1]Techical University of Crete, School of Mineral Resources Engineering, 73100 Chania, Crete, Greece.

*Corresponding author: Despina Pentari

E-mail: dpentari@tuc.gr, tel: 00302821037619

GRAPHICAL ABSTRACT

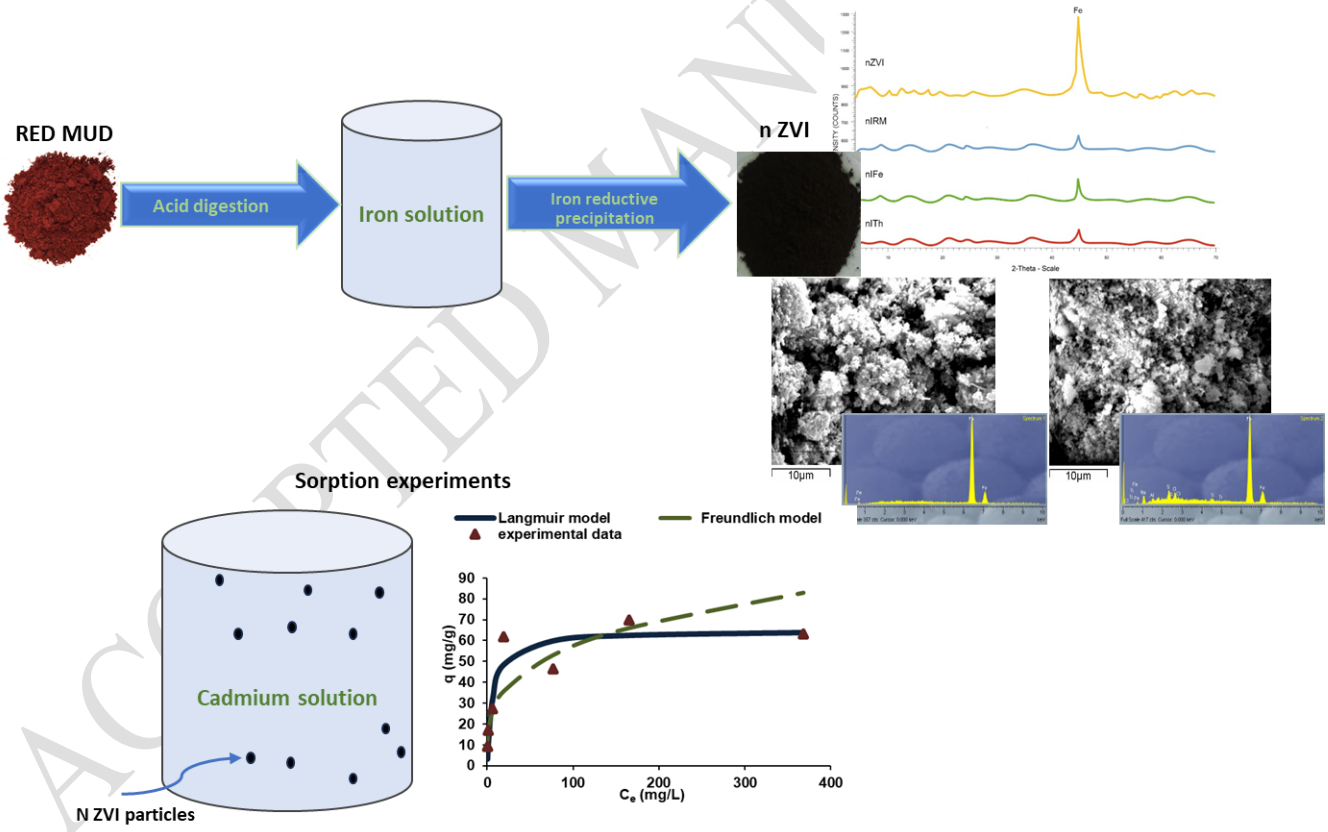

ABSTRACT

The aim of the present study was to synthesize a sorbent material, nanoscale zero valent iron (n ZVI), using red mud as the iron source in the framework of circular economy. The sorbent synthesized was tested for Cd removal from spiked aqueous solutions. For the synthesis of the sorbent, iron reductive precipitation was used. The specific surface area (BET method) of the sorbent prepared was determined, while its surface composition, morphology, and texture were examined by powder X-ray Diffraction (XRD) and Scanning Electron Microscopy (SEM-EDX). The sorption efficiency of the sorbent produced was investigated with kinetic and equilibrium experiments, performed in batch conditions. MATLAB software was used to fit experimental data to Langmuir and Freundlich equations. The results of the study showed that with the described process, nanoscale zero valent iron was prepared with grain size 81 and 89 nm and specific surface area of 36.59 and 28.9 $m^2 \cdot g^{-1}$ depended on the synthesis procedure followed. The sorbent appeared to be efficient for Cd removal from spiked aqueous solutions. Kinetic experiments proved that equilibrium was achieved within 24h while the maximum sorption capacity as evidenced by equilibrium experiments was 65 $mg \cdot g^{-1}$. Data proved to follow the pseudo second order model and to fit better to the Langmuir equation.

Keywords: nano zero valent iron, red mud, bauxite residue, sorption, isotherms, cadmium, circular economy

1. Introduction

In the context of circular economy, recycling and repurposing is of major importance, since it contributes not only to waste reduction but also to the conservation of natural resources. It is in this context that repurposing byproducts or wastes produced by different industrial activities worldwide, has attracted the interest of scientific community. There are, therefore, numerous research works which investigate and propose effective methods to promote waste valorisation. Red mud (RM), or bauxite residue as it is often referred to, belongs to the industry byproducts or wastes that possess

serious and alarming environmental concern and extensive research studies are carried out around the world, in order to explore the potential of its effective utilization (Vilakazi, 2022, Hind, 1999). Red mud is the solid, fine-grained waste material that is produced, by alumina industries, during the refining of bauxite to create alumina (Al_2O_3) through the Bayer process. Bauxite residue is a complex mixture of the original compounds found in the parent material and compounds added or formed during the alumina production process. Its major components are various oxides, including iron, silicon, aluminum, calcium, and titanium oxides, as well as some rare-earth elements (Paramguru, 2005, Matthaiou, 2018, Wang, 2019). It is estimated that producing 1 ton of aluminum generates approximately 1.6–2.5 tons of red mud, depending on bauxite characteristics, while in 2020, annual alumina production, worldwide, was approximately 133 Megatons (Mt), resulting in the production of over 260 Mt of red mud (Paramguru, 2005). Although red mud cannot be considered toxic material, due to its high production rate and high alkalinity, can have a significant environmental impact and its disposal remains a problem to be solved (Power, 2011, Gao, 2022). Research on red mud eco-friendly utilization is expanding into various fields and a number of applications have been proposed aiming to recycle or repurpose it. For instance, such applications include metal recovery, production of various materials including environmentally friendly construction materials, fillers, polymers and ceramics, utilization as a catalyst, a coagulant or a flocculant material as well as fabrication of hydroelectric cells to generate green electricity. In addition, due to its size and elevated specific surface area, numerous studies have focused on its potential for environmental remediation with its performance, as an inexpensive and efficient sorbent to remove organic or inorganic pollutants in various environments, to be thoroughly investigated (Hind, 1999, Paramguru, 2005, Gao, 2022, Oschsenkuehn-Petropoulou, 2018, Liu, 2014, Akcil, 2018, Borra, 2015, Lymperopoulou, 2019, Hatzilyberis, 2020, Davris, 2018, Borra, 2016, Qu, 2013, Dev, 2020).

Nanoscale zero-valent iron (n ZVI) is a nanomaterial that is widely used for soil and ground water remediation (Pedram, 2020, Chen, 2017, Boparai, 2011, Chen, 2011, Ahmadi, 2017, Sahu, 2022, Pang, 2019, Amiri, 2017). Various researchers reported studies on the use of n ZVI for remediation

of heavy metals, including cadmium, (Boparai, 2011, Ahmadi, 2017, Pentari, 2019, Hardijeet, 2011), and a variety of other groundwater pollutants. Despite its numerous advantages, such as high reduction capacity, high efficiency, and low economic and environmental costs, n ZVI comes with some limitations due to its small particle size. To overcome the existing limitations several researchers have proposed the use of a stable support material (Chen, 2011, Ahmadi, 2017, Sahu, 2022, Pang, 2019, Amiri, 2017, Pentari, 2019), and various supporting materials, including red mud (Sahu, 2022), have been proposed.

Heavy metal ions, including cadmium, are released into the environment in a number of different ways and because of their accumulation in living organisms form a serious and complex problem that has been a focus of attention all over the world and strict legislative standards, concerning metals concentration in the environment, have to be met. Cadmium is a heavy metal of significant environmental concern. It has been classified as carcinogen and teratogen that can impact different human organs. It can be released to the environment through various processes including fossil fuels combustion, metal production, electroplating, fertilizers application and batteries and pigments manufacturing. There is, therefore, a considerable interest in developing techniques to remove cadmium from contaminated water. Among the techniques proposed sorption onto nanoscale zerovalent iron is a promising and cost effective one and nanoscale zerovalent iron has been reported to possess high sorption capacities with maximum sorption capacity for Cd^{2+} to be up to 770 $mg \cdot g^{-1}$ at room temperature (Hardijeet, 2011).

The aim of the present study is to investigate the feasibility of preparing nano scale zero valent iron utilizing red mud as the iron precursor. The proposed procedure offers clear advantages since it not only helps in addressing the need for red mud recycling but also results in the synthesis of a high added value material, efficient for environmental remediation, contributing in that way to sustainable development. The synthesized material was tested for the removal of cadmium ions from spiked aqueous solutions with kinetic and equilibrium experiments, performed in batch conditions. For

comparison reasons the characteristics of a sorbent prepared using $FeCl_3$ as the iron source, and commercial n ZVI, was investigated along with the synthesized sorbent.

2. Materials and methods

Red mud used as the iron source to prepare nanoscale zero valent iron in the present study, was provided by the second largest bauxite producer in Europe, Aluminium of Greece, which is located at Agios Nikolaos, Viotia, Central Greece. The major constituents (expressed as metal oxides) of the RM used was Fe_2O_3- 50 %, CaO -19 %, Al_2O_3-14 %, SiO_2-7 %, and TiO_2-6 %. The sample was dried at 100 ◦C overnight and used without further conditioning or treatment.

2.1. SORBENT SYNTHESIS

Nano-scale zero valent iron (n ZVI) was synthesized by iron reductive precipitation, with sodium borohydride, using red mud as the iron precursor. Using this 'bottom-up' method of dropwise addition of $NaBH_4$ aqueous solution to the iron containing solution with continuous stirring, the nano scale sorbents were prepared and the reduction of Fe^{3+}, in liquid-phase, can be expressed as follows:

$$4Fe^{3+} + 3BH_4^- + 9H_2O \rightarrow 4Fe^0 \downarrow + 3H_2BO_3^- + 12H^+ + 6H_2\uparrow$$

The molar ratio of borohydride to ferric iron used was 5:1. This ratio was chosen based on literature research, in accordance with the method described in detail by Wang and Zhang (Wang, 1997). Two iron solutions were used the one prepared after the total dissolution of red mud (total dissolution by acid digestion with a mixture 1:1 con. HCl, HNO_3 in PTF beakers) and another that resulted after treating the previously mentioned solution with thioacetamide to separate iron from coexisting ions like Ca (the red mud solution is treated with thioacetamide, and the iron ions, in alkaline environment, are precipitated as sulfides. The precipitate is dissolved by HCl to prepare the new iron containing solution). The reducing agent (freshly prepared aqueous $NaBH_4$, 108 mg per 100 mL) was added dropwise (20 to 30 drops per minute) to the iron containing solution (~1.0 M Fe^{3+}, depending on the iron solution used) under continuous stirring. A black, rapidly settling down precipitate, was

immediately, after introducing the first few drops of $NaBH_4$ solution, formed followed by liberation of H_2, suggesting successful reduction of ferric iron to Fe. After 30 min of stirring, to ensure complete reduction, the precipitate was separated by vacuum filtration, washed with water and acetone three times to remove excess chemicals, and was vacuum oven-dried at 60 ºC for 24 h. Iron concentration was determined in the remaining solution in order to estimate the iron precipitation yield of the procedure. To analyze the residual concentration of iron electrothermal atomic absorption spectroscopy (GF-AAS) was employed. The spectrometer used was the HGA 800-Analyst 100 model by Perkin Elmer. The synthesized sorbents were stored in airtight brown glass containers until used for characterization and sorption experiments. For comparison purposes, following the same procedure, a third sorbent using a solution containing iron chloride (1.0 M $FeCl_3$) was also prepared. Ultrapure, deionized, deoxygenated water (sparged with nitrogen) was used to prepare aqueous solutions and the synthesis was conducted using an appropriate experimental setup maintaining an O_2-free environment by purging with O_2-free nitrogen. All reagents used were of analytical grade, purchased from Sigma Aldrich, Steinheim (Germany). Therefore, with the procedure described above, three sorbents were synthesized, namely n IFe, n IRM, and n ITh using ferric chloride solution, red mud solution and thioacetamide - treated red mud solution respectively.

2.2. SORBENT CHARACTERIZATION

The specific surface area of the sorbents synthesized was determined with the Nova 2200 apparatus (QuantChrom) according to the BET (Brunauer Emmet Teller) method. The mineralogy of the sorbents was determined by X-ray diffraction (XRD) using a Siemens D500 XRD instrument. The data were obtained at 35 kV and 35 mA, with a graphite monochromator, using CuKa radiation. The qualitative evaluation of the data was done with the Software Diffrac Plus by SOCABIM. The quantitative analysis was carried out by the Rietveld Method and Scherrer equation (Langford, 1978) was used to calculate the grain (crystallite) size of the synthesized materials using the line broadening at half the maximum intensity (Full Width at Half Maximum FWHM). Morphology, texture, and composition of the samples were studied by scanning electron microscopy (SEM - EDX) using the

Jeol 5400 instrument equipped with an energy dispersive X-ray analyzer (INCA energy 300). High vacuum evaporation (JEE-4X, Jeol) was applied to form a thin carbon film to make the surface of the specimens electrically conductive.

2.3 SORPTION EXPERIMENTS

The sorption efficiency of the sorbent n ITh, since this is the one proved to possess better characteristics compared to n IRM and similar to those of n IFe, was investigated with kinetic and equilibrium studies with cadmium as the sorbate. For comparison purposes equilibrium experiments were also carried out for sorbent n IFe. The experiments were conducted in batch mode using cadmium spiked, aqueous solutions and the effect of contact time, and metal initial concentration on the sorption process were studied. All experiments were carried out in duplicate at room temperature (25 ± 2 ◦C) with the sorbent dosage to be 0.5 g of sorbent per liter of sorbate solution. Plastic containers capped with Teflon Mininert valves were used, to minimize oxidation of sorbents particles during the experiments. The analysis of cadmium in the solution that was produced after a 48 h treatment of 0.05 g sorbent with 100 mL of deionized water showed that there was no cadmium leaching from the sorbent. In addition, independent blank experiments (no sorbent added) showed that there was no Cd^{2+} sorption to the containers and corresponding caps. The cadmium containing solutions were prepared using analytical grade nitrate salt ($Cd(NO_3)_2$. $4H_2O$) purchased from Sigma Aldrich, Steinheim (Germany). A stock solution containing 1000 mgL^{-1} cadmium was prepared and consequently, the cadmium solutions required for the various experiments were prepared, from the stock solution, by the appropriate dilution.

Initial pH and pH throughout the experiments were determined using a pHmeter (model InolabLevel1, by WTW). pH fluctuated throughout the experiments around 5.5 and since this is reported (Ahmadi, 2017, Sahu, 2022, Pentari, 2019, Hardijeet, 2011) to be an optimum pH for several metals, including cadmium, sorption onto several sorbents including n ZVI, no pH adjustment was considered necessary for the conducted sorption experiments.

2.3.1. KINETIC EXPERIMENTS.

Batch kinetic experiments were carried out as described above with solutions of initial cadmium concentration of 100 $mg \cdot L^{-1}$. After different periods of contact time (0.50 h, 0.75 h, 1 h, 2 h, 5 h, 12 h, 24 h, 48 h, and 72 h) the aqueous phase was withdrawn and the filtered resulting solution was used to determine the residual metal concentration. The residual concentration of cadmium in the aqueous phase was analyzed by electrothermal atomic absorption spectroscopy (GF-AAS). The spectrometer used was the HGA 800-Analyst 100 model by Perkin Elmer. To analyze the experimental data of the sorption kinetics the pseudo-first order and pseudo-second order kinetic models, as shown in equations 1 and 2 respectively, were used

$$\frac{dq_t}{dt} = k_1(q_e - q_t)$$ (eq 1 Pseudo-first order)

$$\frac{dq_t}{dt} = k_2(q_e - q_t)^2$$ (eq 2 Pseudo-second order)

where k_1 (min^{-1}) is pseudo-first order and k_2 ($g \cdot mg^{-1} \cdot min^{-1}$) pseudo-second order rate constants and q_e and q_t sorption capacities at equilibrium and time t. These models have widely been applied and serve as a useful tool in studying processes as the cadmium sorption investigated in the present study, that is metal sorption on heterogenous surfaces. (Sahu, 2022, Hardijeet, 2011).

2.3.2. EQUILIBRIUM EXPERIMENTS.

Sorption isotherm studies were conducted by varying the cadmium initial concentration from 5 to 400 $mg \cdot L^{-1}$ (5, 10, 20, 50, 100, 200, and 400 $mg \cdot L^{-1}$). The sorption conditions were kept the same as in sorption kinetics and 24 h was chosen as contact time. This time interval was chosen because in previous kinetic experiments it was proved to be sufficient to reach equilibrium. The residual concentration of cadmium in the aqueous phase was determined by electrothermal atomic absorption spectroscopy (GF-AAS) as described for the kinetic experiments.

The percent removal and sorption capacity (mg Cd sorbed per g of sorbent) q_e were calculated. For sorption capacity the following equation was used:

$$q_e = (C_0 - C_e)\frac{V}{m_s}$$

where C_o (mg L^{-1}) and C_e (mg L^{-1}) are the Cd^{2+} initial and equilibrium concentrations V (L) is the volume of the Cd^{2+} solution used, and m_s (g) is the sorbent mass added to the solution.

The sorption capacity of the sorbents n IFe, n ITh was calculated and for a nonlinear regression, MATLAB software was used to to test the fitting of experimental equilibrium data to Langmuir (Langmuir, 1918) and Freundlich (Freundlich, 1926) isotherms model as given in the following equations:

$q = q_{max}\, b\, C_e / (1 + b\, C_e)$ (Langmuir)

$q = K\, C_e^{\,1/n}$ (Freundlich)

where q is the amount of cadmium adsorbed per unit mass of sorbent, C_e is the cation concentration at equilibrium, q_{max} is the maximum sorption capacity; K is related to the sorption capacity and b, and n are constants related to sorption intensity.

3. Results and Discussion

3.1. SORBENT CHARACTERIZATION

The grain size and the specific surface area (BET method) of the sorbents prepared in the present study are reported on Table 1. The grain size calculated by the Scherrer equation was 54, 89, 81 nm for n IFe, n IRM, and n ITh respectively, with commercial nZVI to exhibit a grain size of 14 nm. The specific surface area measured was 37.22, 28.29, and 36.59 $m^2 \cdot g^{-1}$ for n IFe, n IRM, and n ITh respectively which is within the range (8-115 $m^{2} \cdot g^{-1}$) reported in literature for nanoscale zero valent iron or modified nanoscale zero valent iron (Sahu, 2022, Liu, 2016, Liu, 2017, Lou, 2019)). The prepared sorbents possess a grain size within the nano scale (<100 nm) with their size to be 3.8 times (n IFe) to 6.4 times (n IRM) higher than that of commercial n ZVI. It is obvious that among the sorbents prepared, n ITh appears to possess better specific surface area and grain size, suggesting that

it could possess a better sorption capacity, than n IRM, similar to the respective characteristics, that was measured for n IFe. This could be attributed to the removal, by the thioacetamide treatment, of metals like Ca from the iron solution prior to being used for the synthesis of the sorbent.

The XRD patterns of the sorbents prepared are presented in Figure 1. It is observed that no crystalline phases co-exist with iron in the samples analyzed, with a strong reflection at 45 ^{0} (2θ) for the commercial n ZVI and the corresponding diffraction peaks at the same position for the prepared sorbents. Scanning electron microscopy was applied to further examine the morphology of the three sorbents and representative images at the same magnification (10 μm) are illustrated in Fig. 2 a, b, and c. It is observed that the sorbents n IFe and n ITh possess a similar morphology where the iron porous material appears to have an irregular, roughly globular structure. The sorbent n IRM appears slightly different exhibiting the form of a more aggregated porous material. Apart from morphology, the composition of the sorbents was also investigated and corresponding EDS spectra of the prepared sorbents are also illustrated in Figure 2a, b, and c. It is obvious, since no prominent peaks of other elements can be detected, that iron is the major constituent of the prepared sorbents and that the thiacetamide treatment of the red mud solution was successful in removing calcium, something that was also confirmed by the ICP-MS analysis of the two red mud solutions.

3.2. SORPTION EXPERIMENTS

3.2.1. KINETIC EXPERIMENTS

The cadmium removal, by the sorbent, as a function of contact time is presented in Figure 3. The kinetic experiments results showed that sorption capacity increased rapidly with increasing contact time while the equilibrium was achieved within 24 h. The rapid sorption of cadmium at the initial stage (0–1 h) can be attributed to a considerable number of empty binding sites at the surface of the adsorbent. Such behavior is reported in literature and it appears that after intense initial sorption, there may be a repulsive force between the solute molecules present on the solid and bulk phases, resulting in slower sorption (Sahu, 2022, Massoudinejad, 2015, Ho, 2006). It could be also concluded that, after 24 h, the binding sites must have been exhausted and no further increase of the sorption capacity

was observed. Thus 24 h appear to be the optimum contact time for the following equilibrium experiments. Kinetics revealed a maximum sorption capacity of 60 $mg \cdot g^{-1}$ at 24 h and described experimental conditions. In Table 2 the rate constants, sorption capacities and corresponding correlation coefficients (R^2) for the two models are reported. Based on the higher R^2, the experimental data of the present study appear to better fit the pseudo second order model implying that the cadmium sorption onto the sorbent prepared for the present study, can be described as chemisorption involving valency forces through mutual sharing or exchange of electron between the sorbent and sorbate such as covalent forces and ion exchange (Ho, 2006).

3.2.2 EQUILIBRIUM EXPERIMENTS

The results of the equilibrium experiments are illustrated in Figure 4. The sorption isotherm may be considered of H or L type according to the classification of Giles et al. (Giles, 1974), indicating that the synthesized sorbent, at the investigated experimental conditions, exhibits high affinity for cadmium. To analyze the experimental equilibrium data the Langmuir and Freundlich models have been applied and MATLAB software was used to test the fitting of experimental equilibrium data to the above-mentioned equations. On Figure 4 both Langmuir and Freundlich fits for Cd are illustrated and on Table 3 the constants qmax and b, and K and n, for Langmuir and Freundlich equations respectively are reported along with the corresponding correlation coefficient. It can be concluded that experimental data of the present work were better fitted to the Langmuir equation than the Freundlich one, since the correlation coefficient calculated for the Langmuir equation was higher than that for the Freundlich equation (Table 3). It can, therefore, be suggested that the cadmium sorption by the synthesized sorbent follows the Langmuir model implying that there is a finite nature of the number of sorbent sites and that the sorption process could be described by the formation of a monolayer coverage of the sorbate on sorbent surface. The maximum sorption capacity calculated by the Langmuir equation is 65 $mg \cdot g^{-1}$. This sorption capacity being inferior to sorption capacities reported for n ZVI (Hardijeet, 2011), is comparable to those reported in literature for various cadmium sorbents and higher, in several cases, than sorption capacities reported for other waste material-based

sorbents (Ahmadi, 2017, Pentari, 2019, Chen, 2011). Equilibrium experiments that were carried out, for comparison purposes, with n IFe sorbent yielded similar results. In the case of n IFe experimental data were better fitted to the Langmuir model and the maximum sorption capacity of the sorbent, calculated by the Langmuir equation, was 69 $mg \cdot g^{-1}$.

4. Conclusions

The results of the present study showed that with the proposed procedure, using red mud as the iron source, nanoscale zero valent iron was successfully prepared, leading to the synthesis of an effective sorbent for cadmium removal from spiked aqueous solutions. The grain size of the sorbents synthesized was within the nano scale, 81 nm and 89 nm for, n IRM, and n ITh respectively, and the specific surface area measured was 28.29, and 36.59 $m^2 \cdot g^{-1}$ for, n IRM, and n ITh respectively, which is within the range (8-115 $m^2 \cdot g^{-1}$) reported in literature for nanoscale zero valent iron or modified nanoscale zero valent iron. Those characteristics were also comparable to the ones measured for the sorbent n IFe which was prepared for comparison purposes using iron (III) chloride. Size, specific surface area, morphology and composition of the sorbent n ITh synthesized, was similar to the respective characteristics of sorbent n Ife something that should be attributed to the removal, by the thioacetamide treatment, of metals like Ca from the iron solution prior to being used for the synthesis of the sorbent. The kinetic experiments showed that equilibrium was achieved within 24 h and the experimental data of the present study appear to better fit the pseudo second order model implying that the cadmium sorption onto the sorbent prepared, can be described as chemisorption involving valency forces through mutual sharing or exchange of electron between the sorbent and sorbate such as covalent forces and ion exchange. The maximum sorption capacity calculated by the Langmuir equation was 65 $mg \cdot g^{-1}$. The attained sorption capacity is comparable to those reported in literature for different cadmium sorbents and higher than sorption capacities exhibited by other waste-based materials that have been proposed as cadmium sorbents. The experimental data of the present work were better fitted to the Langmuir equation than the Freundlich one suggesting that the cadmium

sorption by the synthesized sorbent could be described by the formation of a monolayer coverage of the sorbate on sorbent surface.

Table 1. The grain size (nm) and specific surface area ($m^2 \cdot g^{-1}$) of the sorbents synthesized.

	Grain size (nm)	**Surface area ($m^2 \cdot g^{-1}$)**
n IFe	54	37.22
n IRM	89	28.29
n ITh	81	36.59

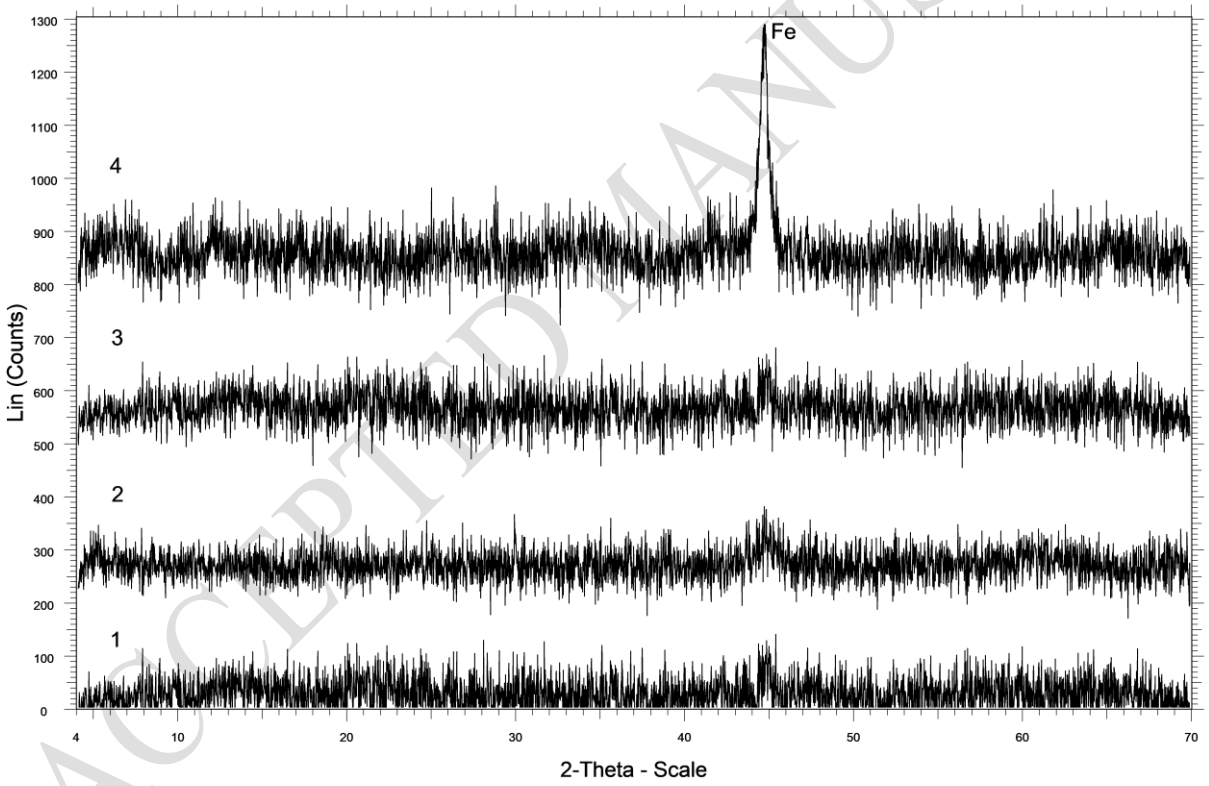

Figure 1. The XRD patterns of the three synthesized sorbents: nITh (1), nIFe (2), nIRM (3), and commercial n ZVI (4).

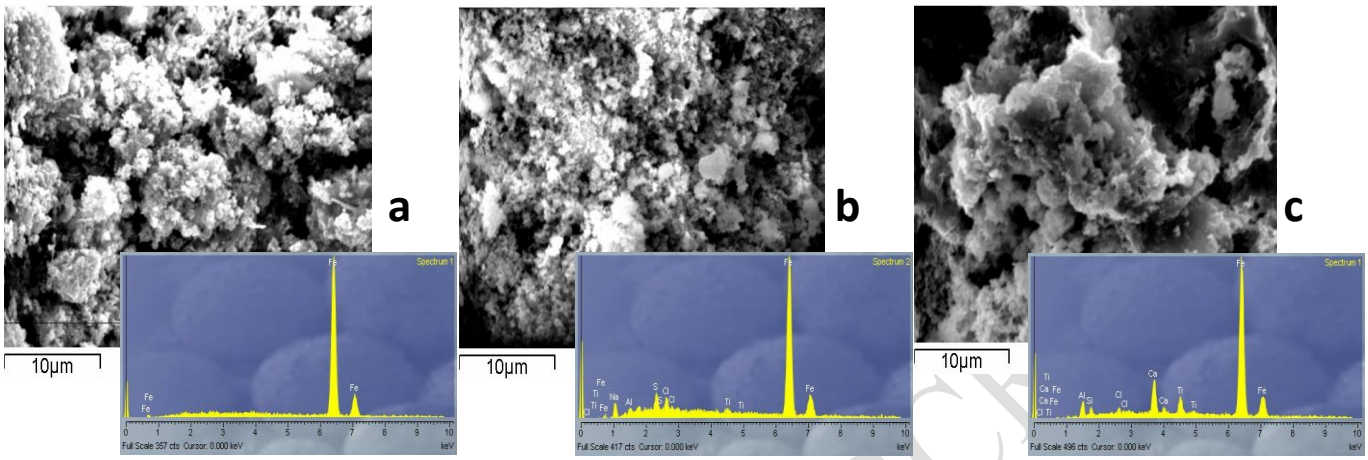

Figure 2. (a), (b), and (c) SEM images of sorbents n IFe, n ITh, and n IRM respectively and corresponding EDS spectra.

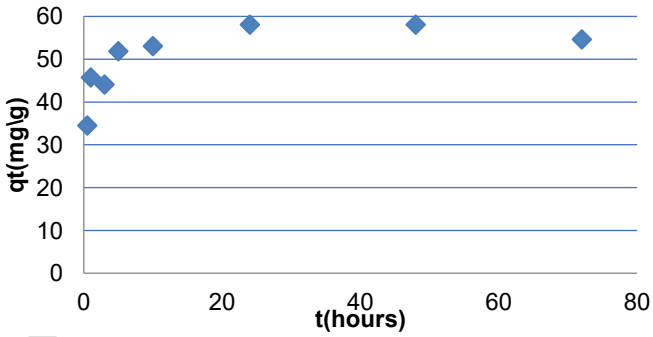

Figure 3. Sorption kinetics of cadmium sorption by the sorbent n ITh. Experimental conditions: sorbent dosage 0.5 g per L, pH 5.5, Temperature 25 ± 2 ◦C and Cd initial concentration 100 mg·L$^{-1.}$

Table 2. Kinetic parameters (constant rate, sorption capacity) and corresponding correlation coefficients for Cd removal by n ITh.

	K	q_{max} $mg{\cdot}g^{-1}$	R^2
Pseudo first order	0.26 h	21.4	0.935
Pseudo second order	0.03 g·mg^{-1} ·h^{-1}	58.8	0.999

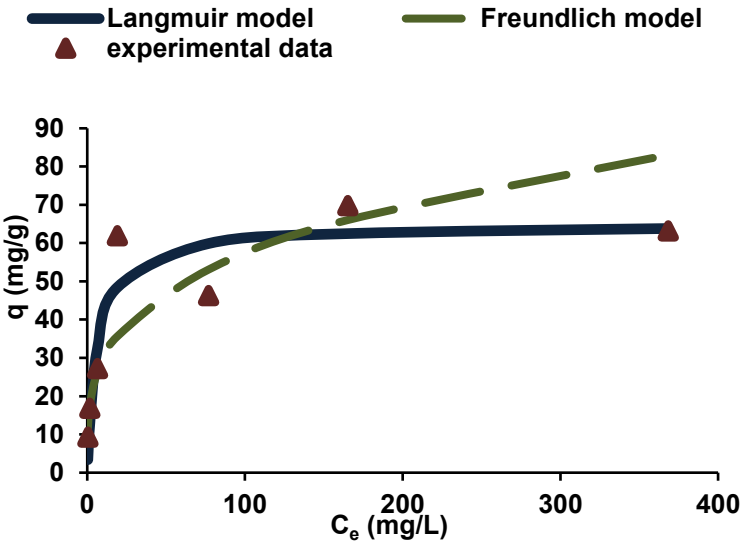

Figure 4 Sorption isotherms: predicted data vs experimental data. Experimental conditions: sorbent dosage 0.5 g per L, pH 5.5, Temperature 25 ± 2 ◦C, time 24 h.

Table 3. Langmuir and Freundlich constants from sorption isotherms and corresponding correlation coefficients for Cd removal by n ITh.

Langmuir			**Freundlich**		
q_{max} mg·g^{-1}	**b** L·mg^{-1}	R^2	**K**	**n**	R^2
65	0.154	0.999	15.35	3.5	0.873

References

Ahmadi M., Foladivanda M., Jaafarzadeh N., Ramezani Z., Ramavandi B., Jorfi S. and Kakavandi B. (2017), Synthesis of chitosan zero-valent iron nanoparticles-supported for cadmium removal: characterization, optimization and modeling approach, *Journal of Water Supply Research and Technology-aqua,* **66**, 116–130.

Akcil A., Akhmadiyeva N., Abdulvaliyev R. and Abhilash M.P. (2018), Overview on extraction and separation of rare earth elements from red mud: Focus on scandium, *Mineral Processing and Extractive Metallurgy Review***, 39**, 145–151.

Amiri M.J., Abedi-koupai J. and Eslamian S. (2017), Adsorption of Hg (II) and Pb (II) ions by nanoscale zero valent iron supported on ostrich bone ash in a fixed-bed column system, *Water Science & Technology,* **76**, 671–682.

Boparai H.K., Joseph M. and O'Carroll D.M. (2011), Kinetics and thermodynamics of cadmium ion removal by adsorption onto nano zerovalent iron particles, *Journal of Hazardous Materials,* **186**, 458–465.

Borra C.R., Mermans J., Blanpain B., Pontikes Y., Binnemans K. and Van Gerven T. (2016), Selective recovery of rare earths from bauxite residue by combination of sulfation, roasting and leaching, *Minerals Engineering,* **92**, 151–159.

Borra C.R., Blanpain B., Pontikes Y., Binnemans K. and Van Gerven T. (2015), Smelting of bauxite residue (red mud) in view of iron and selective rare earths recovery, *Journal of Sustainable Metallurgy,* **2**, 28–37.

Chen X., Ji D., Wang X. and Zang L. (2017), Review on nano zerovalent iron (nZVI): from modification to environmental applications, *IOP Conf. Series: Earth and Environmental Science,* **51**, 12004.

Chen Z., Jin X., Chen Z., Megharaj M. and Naidu R. (2011), Removal of methyl orange from aqueous solution using bentonite-supported nanoscale zero-valent iron, *Journal of Colloid and Interface Science,* **363**, 601–607.

Davris P., Marinos D., Balomenos E., Alexandri A., Gregou M., Panias D. and Paspaliaris I. (2018), Leaching of rare earth elements from 'Rödberg'ore of Fen carbonatite complex deposit, using the ionic liquid HbetTf2N, *Hydrometallurgy,* **175**, 20–27.

Dev S., Sachan A., Dehghani F., Ghosh T., Briggs B.R. and Aggarwal S. (2020), Mechanisms of biological recovery of rare-earth elements from industrial and electronic wastes: A review, *Chemical Engineering Journal*, **397**, 124596–124613.

Freundlich H, *Colloid and Capillary Chemistry,* Metheum and Co. Ltd., London **1926** 883.

Gao J., Qu X., Lan X., Li Y. and Guo Z. (2022), A green method for solidification and recovery of soluble sodium in red mud via super-gravity, *Process Safety and Environmental Protection*, **161**, 384–391.

Giles C.H., Smith D. and Huitson A. (1974), A general treatment and classification of the solute adsorption isotherm, *Journal of Colloid and Interface Science,* **47**, 755-766.

Hatzilyberis K., Tsakanika L.A., Lymperopoulou T., Georgiou P., Kiskira K., Tsopelas F., Ochsenkühn K.M. and Ochsenkühn Petropoulou M. (2020), Design of an advanced hydrometallurgy process for the intensified and optimized industrial recovery of scandium from bauxite residue, *Chemical Engineering and Processing: Process Intensification*, **155**, 108015–108033.

Hind A.R., Bhargava S.K. and Grocott S.C. (1999), The surface chemistry of Bayer process solids: a review**,** *Colloids and Surfaces*, **146**, 359–374.

Ho Y-S. (2006), Review of second-order models for adsorption systems, *Journal of Hazardous Materials,* **136**, 681-689.

Langford J. I. and Wilson A. J. C. (1978), Scherrer after sixty years: A survey and some new results in the determination of crystallite size *Journal of Applied Crystallography*, **11**, 102-113.

Langmuir I. (1918), The adsorption of gases on plane surfaces of glass, mica and platinum, *Journal of American Chemical Society,* **40**, 1361-1403.

Liu T., Yang Y., Wang Z.L. and Sun Y. (2016), Remediation of arsenic (III) from aqueous solutions using improved nanoscale zero-valent iron on pumice, *Chemical Engineering Journal,* **288**, 739–744.

Liu H., Li M., Chen T., Chen C., Alharbi N.S., Hayat T., Chen D., Zhang Q. and Sun Y. (2017), New synthesis of nZVI/C composites as an efficient adsorbent for the uptake of U(VI) from aqueous solutions, *Environmental Science and Technology,* **51**, 9227–9234.

Liu Y. and Naidu R. (2014), Hidden values in bauxite residue (red mud): Recovery of metals, *Waste Management,* **34,** 2662–2673.

Lou Y., Cai Y., Tong Y., Hsieh L., Li X., Xu W., Shi K., Shen C., Xu X. and Lou L. (2019), Interaction between pollutants during the removal of polychlorinated biphenyl heavy metal combined pollution by modified nanoscale zero-valent iron, *Science of Total Environment*, **673**, 120–127.

Lymperopoulou T. Georgiou P., Tsakanika L.A., Hatzilymperis K. and Ochsenkühn-Petropoulou M. (2019), Optimizing Conditions for Scandium Extraction from Bauxite Residue Using Taguchi Methodology, *Minerals*, **9** 236–249.

Massoudinejad M., Asadi A., Vosoughi M., Gholami M., Kakavandi B. and Karami M.A. (2015), A comprehensive study (kinetic, thermodynamic and equilibrium) of arsenic (V) adsorption using $KMnO_4$ modified clinoptilolite, *Korean Journal of Chemical Engineering,* **32**, 2078–2086.

Matthaiou V., Frontistis Z., Petala A., Solakidou M., Deligiannakis Y., Angelopoulos G. N. and Mantzavinos D. (2018), Utilization of raw red mud as a source of iron activating the persulfate oxidation of paraben, *Process Safety and Environmental Protection,* **119,** 311-319.

Ochsenkuehn-Petropoulou M., Tsakanika L.A., Lymperopoulou T., Ochsenkuehn K.M., Hatzilyberis K., Georgiou P., Stergiopoulos C., Serifi O. and Tsopelas F. (2018), Efficiency of sulfuric acid on selective scandium leachability from bauxite residue, *Metals*, **8,** 915-1031.

Pang H., Diao Z., Wang Xiangxue, Ma Y., Yu S., Zhu H., Chen Z., Hu B., Chen J. and Wang Xiangke (2019), Adsorptive and reductive removal of U(VI) by Dictyophora indusiate-derived biochar supported sulfide NZVI from wastewater, *Chemical Engineering Journal,* **366**, 368–377.

Paramguru R.K., Rath P.C. and Misra V.N. (2005), Trends in red mud utilization, Review, *Mineral Processing and Extractive Metallurgy,* **26** (1), 1-29.

Pedram H., Hosseini M.R. and Bahrami A. (2020), Utilization of A. niger strains isolated from pistachio husk and grape skin in the bioleaching of valuable elements from red mud, *Hydrometallurgy*, **198,** 105495–105507.

Pentari D. abd Vamvouka D. (2019), Cadmium Removal from Aqueous Solutions Using Nano-Iron Doped Lignite, *IOP Conf. Series: Earth and Environmental Science,* **221,** 012135.

Power G., Gräfe M. and Klauber C. (2011), Bauxite residue issues: I. Current management, disposal and storage practices, *Hydrometallurgy,* **108,** 33–45.

Qu Y. and Lian B. (2016), Bioleaching of rare earth and radioactive elements from red mud using Penicillium tricolor RM-10, *Bioresource Technology,* **136,** 16–23.

Sahu M., K., Patel R. K. and Kurwadkar S. (2022), Mechanistic insight into the adsorption of mercury (II) on the surface of red mud supported nanoscale zero-valent iron composite, *Journal of Contaminant Hydrology,* **246,** 103959.

Vilakazi A.Q., Ndlovu S., Chipise L. and Shemi A. (2022), A Review on Sustainable Developments and Economic Considerations, *Sustainability (Switzerland)*, **14**, no. 4 1958 32.

Wang C.B. and Zhang W.X, (1997), Synthesizing nanoscale iron particles for rapid and complete dechlorination of TCE and PCBs, *Environmental Science and Technology,* **31**, 2154–2156.

Wang L., Sun N., Tang H. and Sun W. (2019), A review on comprehensive utilization of red mud and prospect analysis, *Minerals,* **9** 362-383.